Rare Metal Materials and Engineering
Volume 52, Issue 4, April 2023
Available online at www.rmme.ac.cn

Science Press

Cite this article as: Wu Xiaoming, Shi Changgen, Gao Li, et al. Study on Parameters and Wave Growth Mechanism of Explosive Welding Based on SPH-FEM[J]. Rare Metal Materials and Engineering, 2023, 52(04): 1272-1282.

ARTICLE

Study on Parameters and Wave Growth Mechanism of Explosive Welding Based on SPH-FEM

Wu Xiaoming, Shi Changgen, Gao Li, Li Wenxuan, Feng Ke

Army Engineering University of PLA, Nanjing 210007, China

Abstract: The SPH-FEM coupling algorithm was applied to simulate four typical explosive composite combinations including titanium-steel, stainless steel-steel, copper-steel and titanium-aluminum. The ranges of strain rate applicable to the Johnson-Cook strength equation and the Steinberg-Guinan strength equation were analyzed theoretically. Besides, the effects of the thickness of the flyer plate and base plate, impact velocity and impact angle on the temperature, pressure and microstructure of the interface during explosive welding were investigated. The growth mechanism of the interface wave, vortex and a small amount of splashing molten blocks were explored through numerical simulation. Results show that the interface temperature, pressure and waveform size increase with the rise in flyer plate thickness and impact velocity, while the peak of interface pressure decreases with the increase in impact angle. The change in the thickness of the base plate cannot directly affect the temperature and pressure of the interface, where the material behaves as an incompressible liquid and reciprocates, producing sinusoidal waveforms, vortex, and splash molten blocks.

Key words: explosion welding; interface wave; SPH-FEM; parameter studies; strength equation

As a special processing technology for the production of composite materials, explosive welding technology relies on the enormous chemical energy released from explosion to achieve the high-speed collision between the base plate and the flyer plate, as required for the high-strength solid phase metallurgical bonding[1–3]. Capable of integrating the advantages of dissimilar materials, explosive composite has been widely applied in aerospace, marine ships, chemical production and other fields[4–5]. Through a long time of theoretical development, many scholars explored the effects of explosive welding parameters on welding strength from different perspectives. For example, in 1975, Deribas et al[6] first analyzed the angle of jet formation, the critical impact pressure required for critical jet generation in the range of subsonic velocity, critical flow transition velocity and other parameters, based on which the upper and lower limits of two parameters, impact angle β and impact point movement velocity V_c, were determined. By analyzing the energy conditions of unit area in welding, Wylie et al[7] determined the upper limit of explosive welding impact velocity V_p. Shi et al[8] analyzed the maximum tensile limit of flyer plate at the time of bending deformation under detonation pressure, thus determining the available range of static parameters such as explosive, cladding plate and placement conditions. In view of the problems such as jet formation, welding energy, critical impact pressure, material physical limit, the use range of various parameters was determined to achieve effective composite welding for a large number of dissimilar metals, thus promoting the development of explosive welding technology. However, due to the existence of interfacial impurities such as brittle intermetallic compounds and continuous melting zone, it remains difficult to weld hard and brittle metals, strongly passivated and easily oxidized active metals, as well as the dissimilar metals with clear differences in physical and chemical properties. Therefore, it is necessary to conduct further research on explosive welding parameters[9–11]. In respect of parallel explosive welding, the moving velocity of impact point V_c is equal to explosive detonation velocity V_d. In the practice of explosive welding with specific performance requirements, the type of explosive, flyer plate and base plate materials are pre-determined. The study on explosive welding parameters focuses mainly on

Received date: August 02, 2022
Foundation item: National Natural Science Foundation of China (51541112)
Corresponding author: Shi Changgen, Ph. D., Professor, School of Field Engineering, Army Engineering University of PLA, Nanjing 210007, P. R. China, E-mail: shichanggen1@sina.com

static and dynamic parameters such as impact velocity V_p, impact angle β, flyer plate thickness δ_f and base thickness δ_b.

In fact, the temperature T, pressure P and microstructure of the interface after bonding play the most significant role in the quality of interface welding. The morphology of interface determines the meshing area and form of dissimilar metal contact, which is a hot spot in regard to explosive welding technology[12]. As a precondition for the short-time diffusion of interface elements, high temperature improves the diffusion coefficient, provides energy for the metal atoms to migrate from the original equilibrium position[13], and enhances interface bonding[14–15]. However, an excessively high temperature causes not only the melting, oxidation, ablation and gasification of the material, but also the formation of continuous melting zone, ingot structure and other impurities at the bonding interface of the composite, thus increasing the risk of brittle failure and reducing the bonding strength of the material[16]. In addition, the rate of temperature change has a significant impact on the quality of interface. The rate of temperature change in explosive welding process is over 10^9 ° C/s. Due to the difference in thermal expansion coefficient of dissimilar metals, the expansion shrinkage of materials caused by the rapid change of temperature will also lead to internal defects and generate residual internal stress, thus affecting the applicability of materials[17]. High pressure is conducive to interface bonding, which is a precondition for atoms at the interface to get close enough to achieve mutual attraction[18]. Too low pressure of the materials is not conducive to effective recombination, while too high pressure subjects the electrons on the metal atomic orbit to greater constraints. As the atomic orbital energy increases, which is different from the characteristics of metal oxidation under normal pressure[19], heterogeneous intermetallic compounds are generated, microcracks develop at the interface and the weld is damaged.

Due to the particularity of explosive welding, it is difficult to capture the interface temperature T, pressure P and interface growth in the welding process. As a result, it is almost impossible to conduct study on the temperature, pressure and morphology of the interface. In view of few studies on interface temperature and the characteristics of pressure as well as the inconclusive mechanism of interface wave formation, a theoretical analysis was conducted in this study to determine the advantages of Steinberg-Guinan strength equation over the Johnson-Cook strength equation. SPH-finite element method (FEM) coupling algorithm was used to simulate four typical combinations of explosive composite for dissimilar metals under different impact angle β, impact velocities V_p, and thicknesses of flyer plate δ_f, including titanium-steel with high corrosion resistance, stainless steel-steel, titanium-aluminum with light and high strength, and copper-steel with good lubrication and electrical conductivity. The interface was highly consistent with the experimental results, and the whole growth process of interface waveform was observed. Based on the obtained interface temperature and pressure data, the impact of dynamic and static parameters of explosive welding core on interface temperature and pressure and waveform growth was analyzed, thus contributing to further improvment in interface quality and solution of the existing problems about the welding of dissimilar metal.

1 Numerical Simulation of Explosive Welding

1.1 SPH-FEM coupling algorithm

Currently, parallel explosive welding is one of the most widely used methods for layered explosive welding. As shown in Fig. 1, the high pressure generated by explosive explosion makes flyer plate at the point of detonation bend and tilt. Then, it collides with the base plate at the impact velocity V_p, and the direction of the impact velocity V_f is perpendicular to the angular bisector of the impact angle β. Based on this principle, the high-speed tilt collision model of explosive welding is commonly used in the numerical simulation of explosive recombination for various dissimilar metals[20–22]. At present, the major algorithms applied for the numerical simulation of explosive welding include Lagrange, Euler, ALE and SPH[23-26]. As the first and most widely used algorithm, Lagrange algorithm has advantages of high speed of operation and simplicity in calculation. However, Lagrange method requires the mesh to be divided on the material, which makes it impossible to carry out numerical simulation for significant deformation. The Euler and ALE algorithms fill the material into the mesh, thus meeting the calculation requirements for severe plastic deformation, but there remains a problem that the accuracy of the two algorithms is insufficient to deal with the interface problem. The study of Ref. [27−28] shows that the smooth fluid particle dynamics (SPH) algorithm achieves a higher accuracy in the calculation of large deformation, spallation and other phenomena, which makes it more suitable for the simulation reproduction of explosive welding interface. However, it is difficult to simulate the actual explosive welding with a relatively large area due to its long operation cycle and large storage space. To resolve the above problems, the SPH-FEM algorithm was proposed in this study. The SPH algorithm was used exclusively for the collision interface, and FEM was used for the rest of the material, as shown in Fig. 2. With the advantages of SPH and FEM combination, the computing power was concentrated on the composite interface with a thickness of 0.5 mm. In case of finite computing force, the computing power is distributed

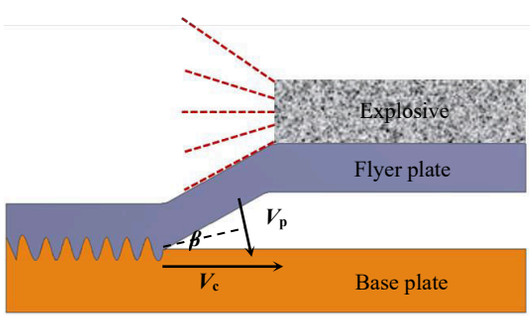

Fig.1 Geometric principle of explosive welding

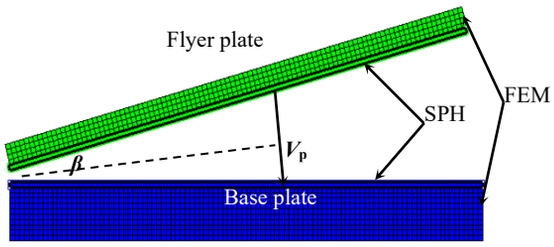

Fig.2 Schematic diagram of high speed oblique impact

across the interface of the joint, so as to improve the accuracy of calculation for the key position and to reduce the overall computing time.

1.2 Johnson-Cook and Steinberg-Guinan Strength Models

As a typical dynamic mechanical behavior, explosive welding involves collision and impact at high temperature, high pressure and high strain rate[1]. At present, the strength equations used to describe the impact and collision behavior of metal materials mainly include Johnson-Cook (J-C) and Steinberg-Guinan (S-G) models. In the J-C strength equation, the yield strength of the material is related to material strain, strain rate and temperature, as shown in Eq. (1).

$$Y = [A + B\varepsilon_p^n][1 + C\ln\varepsilon_p^*][1 - T_H^m] \quad (1)$$

where Y represents the yield stress, ε_p indicates the equivalent plastic strain, ε_p* denotes the normalized equivalent plastic strain rate, T_H means the material temperature control term, A indicates the initial strain, B refers to the hardening constant, C stands for the strain rate constant, n represents the hardening index, and m means the heat softening index.

According to the analysis of Eq. (1), the yield stress is divided into three parts using the J-C model. The first set of parentheses shows the basic change law of stress and strain at room temperature. The second set of parentheses shows the impact of strain rate on the material basic yield stress. The relevant data can be obtained by conducting dynamic mechanical experiments such as Hopkinson pressure bar experiment. The third set of parentheses introduces temperature constraints to the whole equation. When the temperature of the material increases gradually from room temperature, this value approaches zero. When the temperature of the material reaches the same level as the melting point of the material, this value returns to zero; as the yield stress of the material decreases to zero, and the material behaves as fluid.

When the strain rate exceeds 10^5 s^{-1}, however, there are differences between S-G model and J-C model. At this strain rate, the impact of strain rate change on the material yield stress is negligible compared with the effect of thermal softening on yield strength of the material. For the material, its yield stress does not vary with the change in strain rate. Considering the impact of pressure and temperature on the shear modulus of materials, the S-G model is proposed on the basis of Bauschinger effect. The relationship between the yield strength and shear stress of materials at high strain rate is presented as follows:

$$G = G_0\left\{1 + \left(\frac{G'_P}{G_0}\right)\frac{P}{\eta^{1/3}} + \left(\frac{G'_T}{G_0}\right)(T - 300)\right\} \quad (2)$$

$$Y = Y_0\left\{1 + \left(\frac{Y'_P}{Y_0}\right)\frac{P}{\eta^{1/3}} + \left(\frac{G'_T}{G_0}\right)(T - 300)\right\}(1 + B\varepsilon)^n \quad (3)$$

The equation is applicable to $Y_0[1+B\varepsilon]^n \leqslant Y_{max}$. G represents the shear modulus, Y indicates the yield stress, ε denotes the effective plastic strain, and T refers to the temperature. η represents the relative volume, while Y_0, G_0, G'_P, G'_T and P are all constants. Besides, when the temperature exceeds the melting point of the material, the shear modulus and yield stress of the material are treated as 0.

Both of the two strength equations are applicable to the dynamic mechanical behavior of metal at high strain rate and under violent collision. However, welding forming usually occurs within microseconds in the explosive welding process. When the explosive welding interface can be observed, it is possible to capture the adiabatic shear line that occurs only when the strain rate reaches above 10^6 s^{-1} [29]. Therefore, the S-G strength equation can achieve a higher accuracy for the numerical calculation of explosive welding at a strain rate higher than 10^5 s^{-1}.

After the strength model was determined, the Shock state equation was used to determine the relationship between stress, strain and temperature for the dynamic mechanical behavior of the material.

The interface temperature and pressure are closely related to the inherent properties of flyer plate and base plate, the pattern of motion and the setting of explosive welding parameters. To fully understand the influencing factors of interface temperature and pressure, the four explosive composite combinations including titanium-steel, titanium-aluminum, stainless steel-steel, copper-steel were chosen to carry out numerical simulation, and a comparative experiment was performed to determine the accuracy of numerical simulation, thus further ensuring the effectiveness of interface temperature and pressure data.

In numerical simulation, the thickness of flyer plate δ_f was set to 1.5, 3, and 6 mm, while the thickness of base plate δ_b was set to 4, 8, and 12 mm. In other studies, it is indicated that the impact angle β ranges between 5° and 25°[30-31], so as to obtain the ideal interface jet flow and waveform morphology. Therefore, the impact angle β was set to 10°, 15° and 20° for discussion in this study. In addition, the impact velocity V_p was set to 500, 750 and 1000 m/s for each group.

The dynamic parameters of metal materials can be obtained through Hopkinson pressure bar experiment and the parameters used were sourced from ANSYS material database. The parameters used for numerical simulation are listed in Table 1.

2 Results and analysis

2.1 Interface morphology analysis

The morphology of interface is a direct indicator of the bonding form of the dissimilar metal transition interface after explosive welding, which determines the strength of bonding

Table 1 Numerical simulation of material parameters

Specimen	Density/g·cm^{-3}	Gruneisen coefficient	C_1	S_1	β	n	G'_p	G'_T	Y'_p
TA2	4.51	1.23	5.02	1.54	210	0.10	0.50	−2.70	0.010
410S	7.90	1.93	4.57	1.49	43	0.35	1.74	−3.50	0.008
Q345	7.85	1.60	3.98	1.58	2	0.50	1.48	−2.26	0.032
CU	8.93	2.02	3.94	1.49	36	0.45	1.35	−1.80	0.003
AL 1060	2.70	1.97	5.38	1.34	400	0.27	1.77	−1.67	0.003

for the composite. Different from mechanical engagement, explosive welding relies on interatomic interactions as the main source of interface bonding force. In general, the morphology of interface can be classified into three categories: flat, tiny wavy and large wavy. The flat and micro-wavy bond interfaces have fewer defects such as continuous over-melting zone, ingot structure and brittle intermetallic compounds, so it is generally considered as a high-quality bond morphology.

Fig.3 shows the results of numerical simulation and corresponding experimental metallographic results of four dissimilar metal combinations obtained using S-G strength equation and SPH-FEM coupling algorithm. The thickness δ_f of flyer plate is set to 3 mm, the thickness δ_b of base plate is set to 8 mm, impact velocity V_p is set to 750 m/s, and impact angle β is set to 15°. Low-detonation velocity powder emulsion explosives were used for all the experiments. The material composition of the base and flyer plates is shown in Table 2.

The four combinations produce different interface, and the results of numerical simulation are highly consistent with the corresponding results of metallographic experiment, suggesting that the S-G model has a high accuracy in the

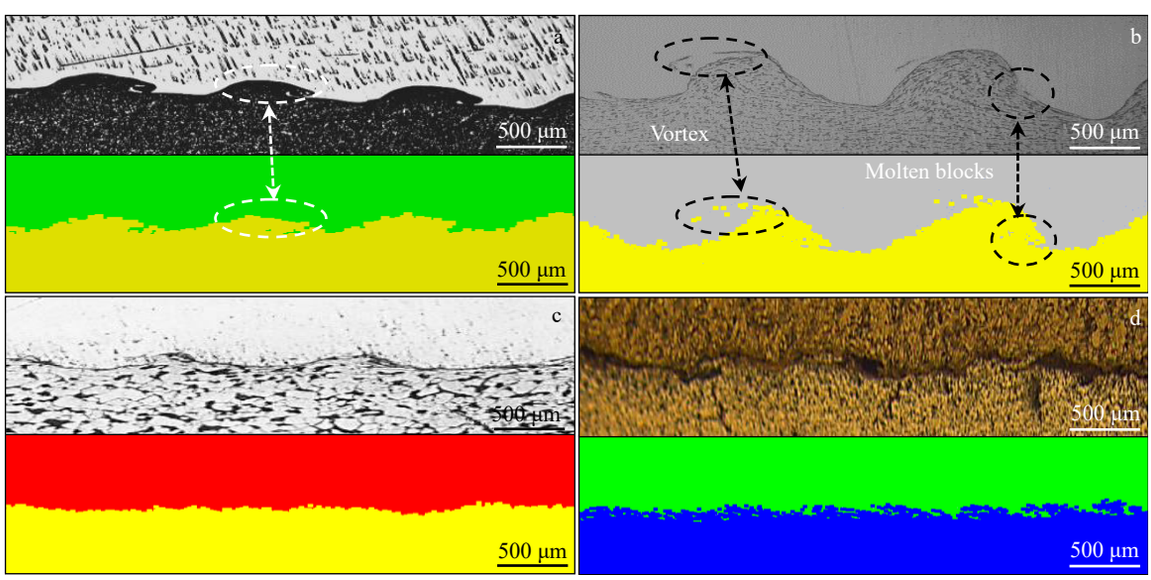

Fig.3 Numerical simulation and metallographic results of four combinations: (a) titanium-steel, (b) stainless steel-steel, (c) copper-steel, and (d) titanium-aluminum

Table 2 Composition of explosive welding experiment materials

Material	Chemical composition/wt%							
Q345R	C	Si	Mn	P	S	Alt	Fe	C
	0.20	0.55	1.20	0.025	0.015	0.020	Residual	0.20
410S	C	Si	Mn	P	S	Cr	Ni	C
	0.08	1.00	1.00	0.04	0.03	11.5	0.60	0.08
AL 1060	Fe	Ti	Al	Si	Mn	Zn	Mg	Cu
	0.35	0.03	Residual	0.25	0.03	0.05	0.03	0.05
H62	Cu	Pb	Sb	Fe	Zn	-	-	-
	0.605	0.002	0.001	0.002	0.395	-	-	-
TA2	Fe	C	N	O	H	Ti	-	-
	0.3	0.1	0.05	0.03	0.015	Residual	-	-

numerical calculation of explosive welding. Fig. 3a shows the explosive composite of titanium-steel. As shown by the ellipse mark, the interface of titanium-steel composite generates periodically high wavelength wave interface with elephant trunk-like wavelet. The average wavelength is 700 μm and its height is 90 μm, and the waveform at this size is typical wavelet morphology. Fig. 3b shows the results of stainless steel-steel, suggesting the formation of a large wavy morphology with a wavelength of 1100 μm and a wave height of about 300 μm at the interface. In addition, there is a small amount of splash melting block and vortex structure captured in the results of experimental and numerical simulation for stainless steel-steel, which are also common morphology of explosive welding interface and have a considerable impact on the bonding quality of materials. Fig. 3c shows the results of copper-steel. The flat wavy interface generated by the explosive composite is defined as the direct bonding morphology by some scholars, and the interface of Ti-Al composite is different from other three combination cases, in which there is no wave shape and the interface is clearly irregular (Fig. 3d). The results of numerical simulation are highly consistent with the experimental results, which verifies the computational accuracy of SPH-FEM algorithm, material shock and S-G model. Moreover, it can be seen clearly in Fig. 3 that the numerical simulation waveforms vary significantly given the same static and dynamic parameters. In fact, the closer the strength, hardness and other physical and chemical properties of the two metals, the more significant the interface waveform effect, and the higher the wave height and wavelength. In addition, the greater the difference in physical and chemical properties, the more significant the difference in deformation tendency of the flyer and base plates in the mechanical and plastic deformation stage and the thermal expansion and contraction stage of heating and cooling, which are mutually affected. Therefore, it is difficult for the interface to generate waveform morphology, which explains why the waveform of steel and stainless steel is obvious, and why the titanium-aluminum composite interface with a clear difference in strength, hardness and the coefficient of thermal expansion shows evident irregularity.

As the most important influencing factor for the bonding quality of explosive welding, interface morphology, especially waveform morphology, has always been the focus of research on explosive welding. Due to the short action time of explosive welding, it is practically difficult to capture the growth process of interface waveform through traditional experimental research, so the mechanism of waveform growth can be studied only based on the interface morphology. At present, there are four major mechanisms of interface growth identified, namely, bahrani engraving mechanism[32], Helmholtz instability mechanism[33], vortex shedding mechanism[34] and stress wave instability mechanism[35].

According to bahrani engraving mechanism, the pressure near the impact point far exceeds the dynamic yield limit of the material, and the interface material is similar to the incompressible inviscid fluid. However, this theory ignores the existence of the interface jet, which is unreasonable. The vortex shedding mechanism is the most similar to the experimental interface waveform, but there is a lack of disturbance obstacle. The remaining two theories are debatable because they are unable to justify the vortex and splash melting block morphology.

The typical characteristics of ideal waveform, interface vortex and a small amount of splashing melting block were obtained through the numerical simulation and experiment for stainless steel-steel. The numerical simulation results can be referenced to explore the mechanism of waveform growth.

In Fig. 4, there are 9 segments of the whole interface waveform growth with equal time difference intercepted, and the whole process of interface waveform growth is reproduced completely. From the calculation results, it can be seen clearly that the interface jet consisting of base plate and flyer plate exists throughout the interface growth process.

Fig. 5 shows the growth process of single waveform and the velocity vector diagram of interface particles with vortex and splash melting block. Fig. 5a–5f show the complete process of base plate wave growth, and the circle in Fig. 5e and 5f indicates the splashing melting block and vortex. It can be seen that in the wavy interface with the base plate waveform as reference, the splash melting block serves as the base plate

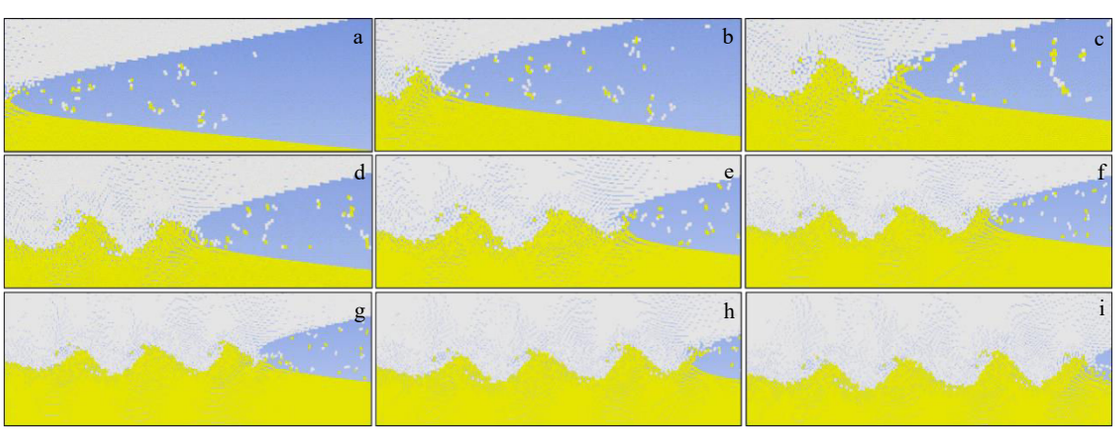

Fig.4 Surface morphology growth process of stainless steel-steel interface intercepted at the same time interval

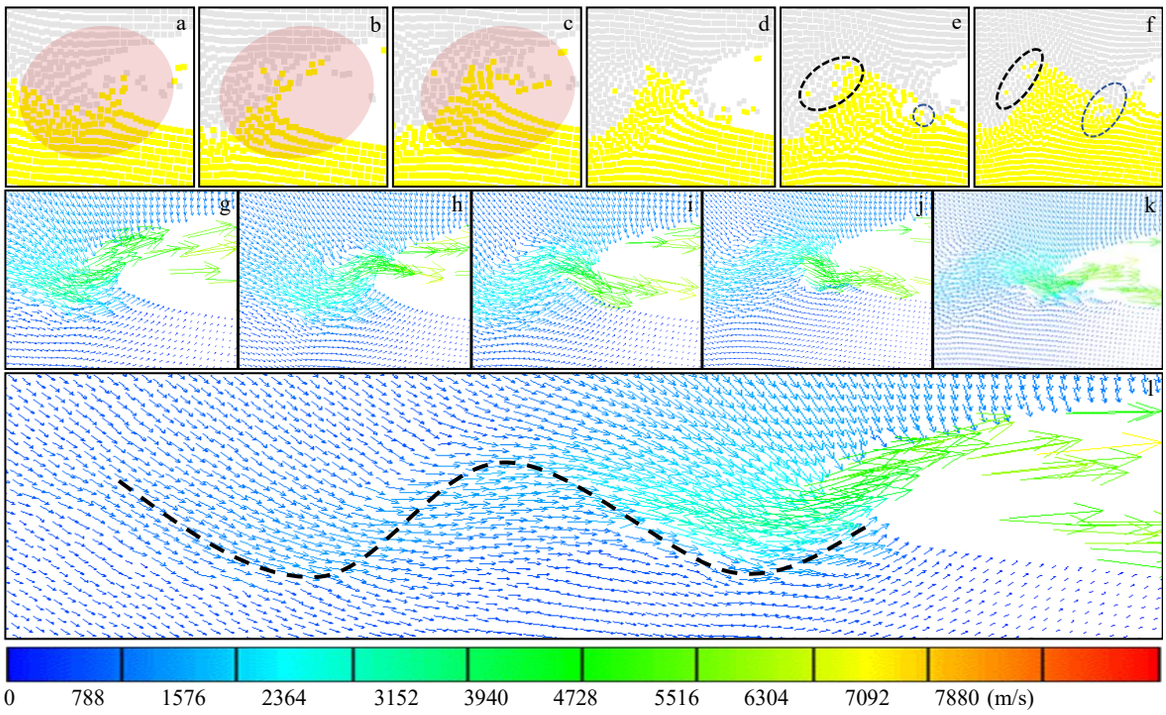

Fig.5 Growth process (a–f) and velocity vector diagram (g–l) of single waveform intercepted at the same time interval

material, and the vortex structure acts as the composite material. According to Fig. 5a–5l, the interface morphology is analyzed. Firstly, the high temperature and high pressure conditions are generated by the high speed inclined collision between the base and flyer plate. The high-speed jet above 4000 m/s is generated by the collision, the material on the surface of the base plate near the collision point exhibits the behavior of incompressible fluid (red area in Fig. 5a–5c), and the surface flow movement of the flyer plate causes initial accumulation for the surface flow of the base plate. Due to the short action time of explosive welding and the limited heating distance in the direction of thickness, the other part of explosive welding remains incompressible solids with high yield strength except the surface metal near the impact point. The flow on the surface of the clad plate is affected not only by the resistance of the base plate in the direction of thickness but also by the resistance of the base plate in front of the impact point. The flow on the surface of the flyer plate shifts upward gradually in the direction of the base plate surface, and the flow on the surface of the base plate accumulates into a wave crest progressively (Fig. 5b and 5c). Consequently, the flow on the surface of the base plate impacts the surface of the flyer plate. Besides, due to the obstruction by the reaction force of the flyer plate material, the flow of the base plate is reversed to form a complete waveform of the base plate. Given the impact between flyer plate flow and base plate flow to flyer plate surface, part of flyer plate flow gets blocked and rotates anticlockwise, thus forming a small amount of splashing molten block morphology with part of base plate flow. After the formation of a complete waveform, part of the flow of flyer plate rotates clockwise to form the wave front vortex when the flow of flyer plate affects the base plate surface again (Fig. 5d–5f). The interface flow (not the interface jet) reciprocates to form a periodic sine wave. As shown in Fig. 5l, the interface metal maintains a velocity of 700–3500 m/s after the collision point gets past, and it continues to grow for a period of time.

Fig. 6 shows the interfacial morphology of four different combinations of explosive welding with different parameters. As revealed by Fig. 6a and 6b, when all other parameters remain unchanged except collision speed V_P or the thickness of the flyer plate δ_f increases, the waveform morphology of the four combined interfaces including titanium-aluminum, titanium-steel, stainless steel-steel and copper-steel becomes increasingly obvious, while the wavelength and wave height increase. However, there is no significant linear correlation between wave size and base plate thickness or impact angle. Changing the thickness of the base plate can have an impact on the waveform morphology interface, but cannot determine the single linear variation law (Fig. 6c and 6d). Despite the difference in the 9 parameter settings of each composite, each composite maintains its own interfacial characteristics. The interface waveform of titanium-steel is dominated by elephant nose shape, while that of stainless steel-steel is evident, which makes it easy for the copper-steel and titanium-aluminum interfaces to form flat or irregular morphology.

The physical and chemical properties of steel and stainless steel are the closest and the interfacial waveform is the most evident[36]. In this study, the conclusions of numerical simulation are verified through the explosive composite experiment of stainless steel and steel. The functional relationship between impact angle β and impact velocity V_P

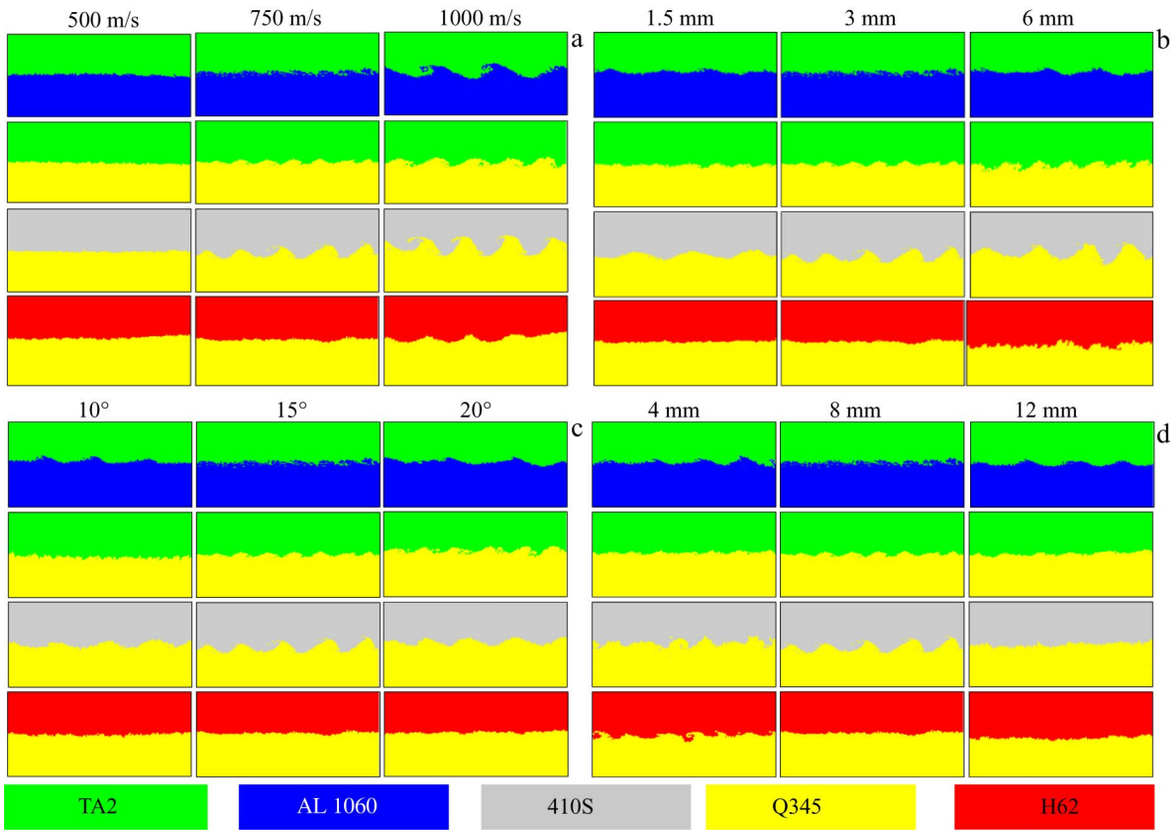

Fig.6 Numerical simulation of interface under different parameters: (a) different collision velocities with β=15°, δ_f=1.5 mm, and δ_b=8 mm; (b) different thicknesses of flyer plate with β=15°, V_p=750 m/s, and δ_b=8 mm; (c) different impact angles with V_p=750 m/s, δ_f=1.5 mm, and δ_b=8 mm; (d) different thicknesses of base plate with V_p=750 m/s, β=15°, and δ_f=1.5 mm

(Eq.(7) and Eq.(8)) can be determined through the synthesis of 1-dimensional Gurney equation of motion (Eq. (4)), Andre Koch[37] charge model (Eq. (5)) and geometric relationship of parallel explosive welding (Eq. (6)). There is a relationship found between impact angle and impact velocity:

$$V_p = 2V_d \sin(\beta/2) \tag{4}$$

Eq.(8) and Eq.(9) are obtained by combining Eq.(4)–Eq.(7). Eq.(8) and Eq.(9) suggest that the impact speed V_p and impact angle β increase with the thickness of the explosive when the material and specification of the flyer plate are determined.

$$V_p = \left(\frac{6ER}{5 + R + 4/R}\right)^{1/2} \tag{5}$$

$$E = \frac{1}{\gamma^2 - 1}\left(\frac{\gamma}{\gamma + 1}\right)^{\gamma} V_d^2 \tag{6}$$

$$R = \frac{\rho_e \delta_e}{\rho_f \delta_f} \tag{7}$$

$$\beta = 2\arcsin\left(\frac{1}{2}\left(\frac{\gamma}{\gamma^2 - 1}\right)^{\gamma/2}\left[\frac{6\rho_e^2\delta_e^2}{(\gamma^2 - 1)\left(5\rho_e\delta_e\rho_f\delta_f + \rho_e^2\delta_e^2 + 4\rho_f^2\delta_f^2\right)}\right]^{1/2}\right) \tag{8}$$

$$V_p = \left(\frac{\gamma}{\gamma^2 - 1}\right)^{\gamma/2} V_d \left[\frac{6\rho_e^2\delta_e^2}{(\gamma^2 - 1)\left(5\rho_e\delta_e\rho_f\delta_f + \rho_e^2\delta_e^2 + 4\rho_f^2\delta_f^2\right)}\right]^{1/2} \tag{9}$$

where E represents the Gurney coefficient of the explosive, γ denotes a multi-index of explosives, ρ_e indicates the explosive density, ρ_f refers to the density of the flyer plate, δ_e means the explosive thickness, and δ_f stands for the thickness of the laminate.

Fig. 7 shows the interfacial metallographic images of stainless steel-steel and the base plate size is the same as the explosives with a thickness of 15, 25 or 35 mm. Each metallograph consists of a stainless steel (410S) duplex at the top and a plain carbon steel (Q345) base plate at the bottom. The ideal interface waveforms are obtained at different positions under three different conditions, confirming that the metals with similar physical and chemical properties are more likely to form wavy bonds. In addition, the experimental results demonstrate clearly that the interfacial waveform size of stainless steel-steel at different positions of flyer plate increases progressively along the direction of detonation, and rises significantly with the increase in explosive thickness. Based on the aforementioned conclusions of numerical simulation, it can be determined that the increase in explosive thickness improves the collision speed V_p during the explosive welding process, which causes a more significant waveform effect on the size of the interface.

2.2 Analysis of interface temperature and pressure

As the power of the whole system, the chemical energy generated by explosive explosion is converted into three

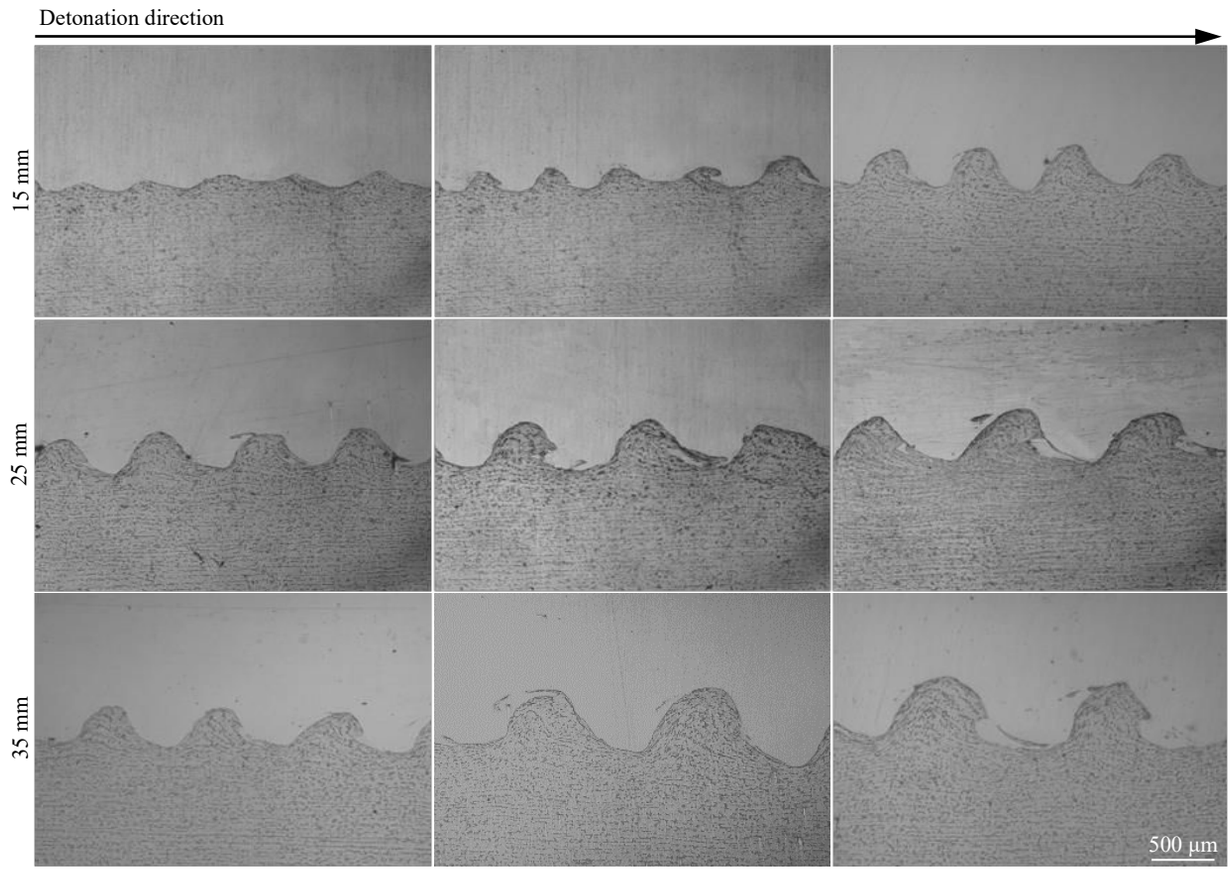

Fig.7 Metallographic images of stainless steel-steel with different explosive thicknesses

forms: detonation, detonation heat and explosive shock wave. The energy, which accounts for a tiny fraction of the whole system, drives the movement of the flyer plate, thus generating the combined initial kinetic energy required for the base plate and the flyer plate. Ref. [16] used completely inelastic collision theory to deduce the quantitative relationship between interface welding energy and parameters such as explosive and flyer plate. It is pointed out that the energy released by the explosive gives the flyer plate the initial velocity (impact velocity). The flyer plate has the initial kinetic energy, and with the increase in the thickness of the flyer plate, the energy used for interface welding increases gradually. When the flyer plate thickness is much higher than the substrate thickness, the flyer plate movement speed is basically unchanged before and after the collision, and the energy of the whole system flows out in the form of the kinetic energy of the composite plate, and cannot be converted into the energy for the interface welding.

With other parameters unchanged, the impact speed V_P and the thickness of the flyer plate δ_f have a significant effect on the kinetic energy obtained by the flyer plate. Fig.8 shows the average interfacial temperature of stainless steel-steel, titanium-steel, titanium-aluminum and copper-steel at different flyer plate thicknesses δ_f and collision speeds V_P. It can be clearly observed that with the increase in flyer plate thickness δ_f or collision speed V_P, the stable temperature shows a significant increase during explosive welding. In addition, the average interfacial temperature except titanium-aluminum explosive bonding is found to be significantly higher than the melting point of the base plate and flyer plate. Based on the analysis of material S-G strength equation, it can be judged that the material at the interface will exhibit a fluid behavior of 0 yield strength and 0 shear strength, which supports the above waveform growth mechanism. As revealed by a further analysis, both titanium and aluminum have high thermal diffusivity due to the high melting point of titanium itself, as a result the temperature of titanium-aluminum explosive welding composite interface is lower than that of material itself and irregular bonding morphology of the interface.

Fig. 9 shows the interface temperature under different impact angles β and base plate thicknesses δ_b. Unlike the change with laminate thickness δ_f and collision velocity V_P, the change of interface temperature is not significant when impact angle and base plate thickness are changed. Because the flyer plate kinetic energy is unchanged, the total energy of the system composed of the base and flyer plate is unchanged when the impact angle β is changed, and the energy used to generate heat during the plastic deformation of the material is basically the same. In the theory of explosive composite window, the impact angle β affects the formation of interfacial jet and prevents the cladding material from bending excessively and causing damage.

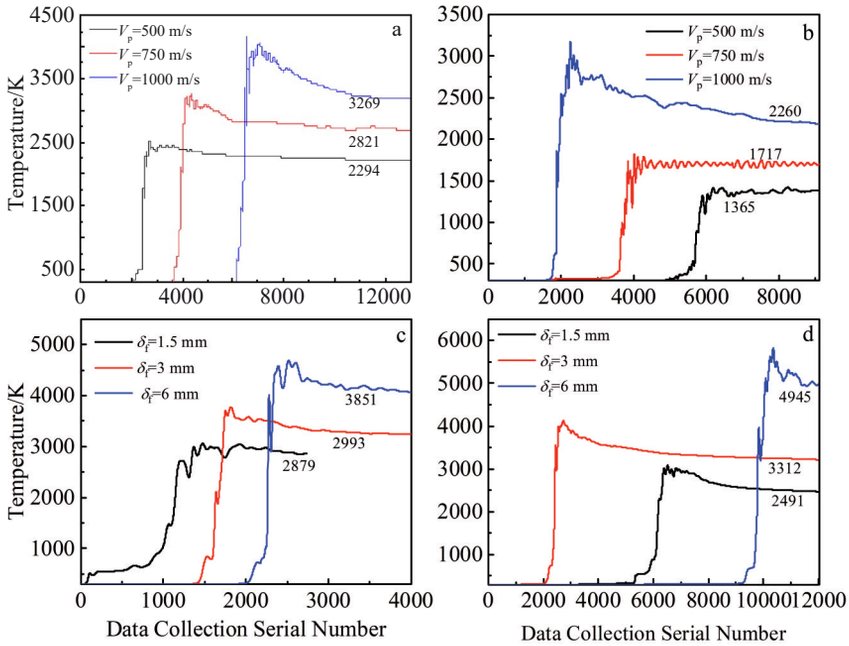

Fig.8 Change of average interface temperature with flyer plate thickness δ_f or impact velocity V_p: (a) titanium-steel, (b) titanium-aluminum, (c) stainless steel-steel, and (d) copper-steel

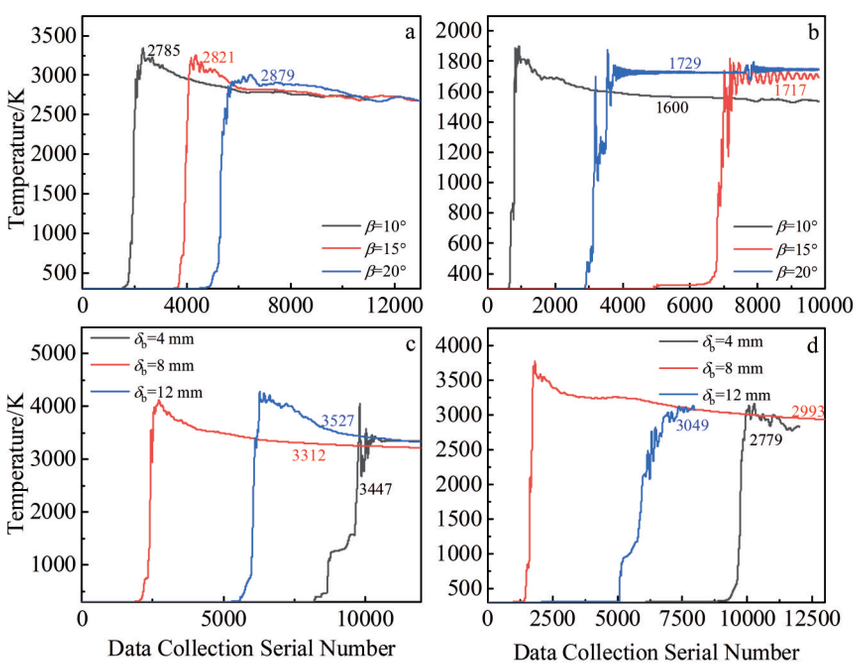

Fig.9 Change of average interfacial temperature with base plate thickness δ_b or impact angle β: (a) titanium-steel, (b) titanium-aluminum, (c) copper-steel, and (d) stainless steel-steel

According to the completely inelastic impact theory, the mass per unit area of the base plate increases when the thickness of the base plate δ_b rises. Under the conservation of momentum, the common velocity mitigates the total kinetic energy loss suffered by the system and the welding energy acting on the interface compound increases. However, the results of numerical simulation show that multiplying the thickness of the base plate δ_b makes no difference to the interface temperature. This is because the mechanical behavior of explosive welding under high pressure and high strain rate leads to a fast welding process and the negligible displacement of the base plate, which is equivalent to the fixed foundation. Therefore, the impact of foundations on tensile reflection waves is discounted in experiment. Both loose sandy foundations which are conducive to the downward movement of the base plate and fixed steel

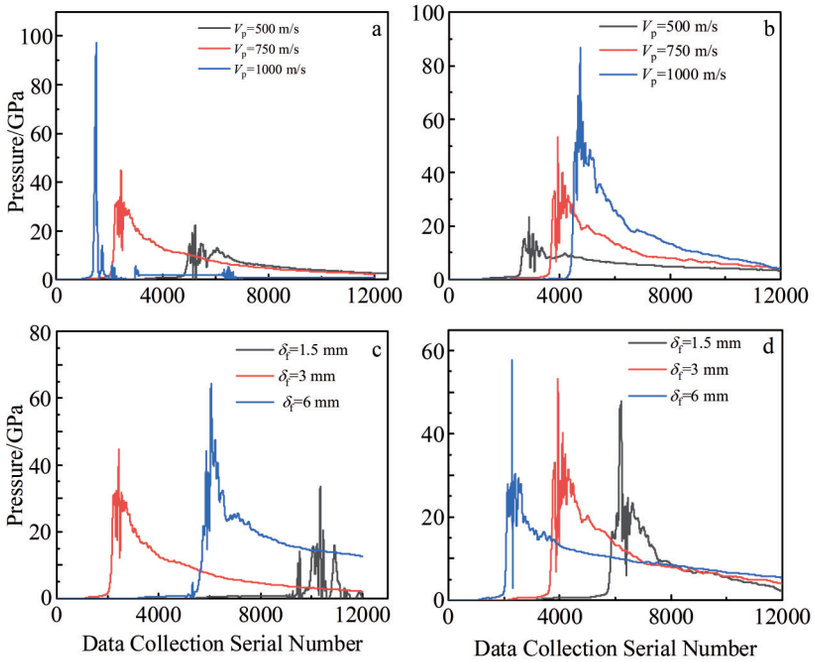

Fig.10 Change of interfacial pressure with flyer plate thickness δ_f or impact velocity V_p: (a, c) copper-steel and (b, d) stainless steel-steel

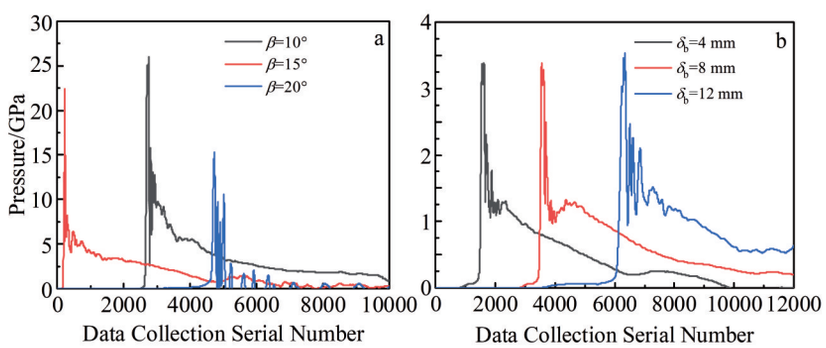

Fig.11 Change of average interfacial pressure with base plate thickness δ_b or impact angle β: (a) titanium-aluminum and (b) titanium-steel

foundations which prevent the downward movement of the base plate can achieve the combination effectively.

Fig. 10 shows the interfacial pressure curves under different thicknesses of flyer plates δ_f and different impact speeds V_P. It can be seen that the interfacial pressure reaches the instantaneous peak between 20 and 100 GPa at the point of impact, and the peak pressure drops immediately after the point of impact is passed. Similar to the pattern of change in interface temperature, the peak value of interface pressure increases with the rise in the thickness of the flyer plate and the impact speed V_P. The interfacial pressure provides the conditions required for the diffusion of interfacial atoms. However, it also makes the material prone to damage. Therefore, it is significant to study the pressure window. Fig. 11 shows the interfacial pressure curves of titanium-aluminum and titanium-steel at different base plate thicknesses δ_b and impact angles β. As base plate thickness δ_b varies, the interfacial pressure peak is basically unchanged. When the impact angle is adjusted, the interfacial pressure drops with the increase in the impact angle.

3 Conclusions

1) The results of numerical simulation for different combinations including titanium-aluminum, titanium-steel, stainless steel-steel and copper-steel are highly consistent with corresponding interfacial micro-morphology obtained from the explosive welding experiment, and the S-G strength model shows high accuracy in the calculation of explosive welding problems. The material waveform with similar physical and chemical properties is more significant. Titanium-steel composite welding is characterized by high wavelet interface, steel-stainless steel shows large wavy bonding morphology, copper-steel interface is flat, and titanium-aluminum interface waveform produces poor effect. The results of numerical simulation show a sharp rise in the size of interface waveform with the increase in the thickness of plate (δ_f and δ_b) and collision speed V_p.

2) The interfacial material behaves as an incompressible

viscous fluid under high temperature and pressure. The wavy interface of explosive welding is due to the reciprocating movement of flyer plate flow and base plate flow. As for the waveform of the base plate, the interfacial vortex is generated by the clockwise movement of the laminar flow and the spattering melting block generated from the counterclockwise movement of the base plate flow.

3) The data obtained by numerical simulation suggest that the temperature and pressure of the interface are positively correlated with the thickness and velocity of flyer plate in explosive welding. The thickness of base plate has little impact on the temperature and pressure of the interface. Increasing the impact angle β is effective in reducing the peak value of the interface impact pressure.

References

1 Loureiro A, Carvalho G H S F L, Galvão Ivan *et al. Advanced Joining Processes*[M]. Netherlands: Elsevier, 2021: 207
2 Findik F. *Materials & Design*[J], 2011, 32(3): 1081
3 Blazynski T Z. *Applied Sciences*[J], 1983(6): 189
4 Vaidyanathan P V, Ramanathan A. *Journal of Materials Processing Technology*[J], 1992, 32(1–2): 439
5 Crossland B. *Explosive Welding of Metals and Its Application* [M]. Oxfords: Clarendon Press, 1982
6 Deribas A A, Simonov V A, Zakharenko I D. *Journal of Materials Processing Technology*[J], 1975, 1: 1
7 Wylie K H. *Explosive Welding; Parameters and Applications*[J], 1969: 48(9): 373
8 Shi C, Ge Y, Shi H *et al. China Welding*[J], 2016, 25(1): 36
9 Inao D, Mori A, Tanaka S *et al. Metals*[J], 2020, 10(1): 106
10 Ren B, Tao G, Wen P *et al. International Journal of Refractory Metals and Hard Materials*[J], 2019, 84: 105 005
11 Saiko V I V, Malakhov A Y, Saikova G R *et al. Inorganic Materials: Applied Research*[J], 2020, 11(2): 448
12 Zeng Xiangyu, Li Xiaojie, Wang Xiaohong *et al. Rare Metal Materials and Engineering*[J], 2020, 49(6): 1977 (in Chinese)
13 Luo Ning, Shen Tao, Xiang Junxiang. *Rare Metal Materials and Engineering*[J], 2018, 47(10): 3238 (in Chinese)
14 Schaefer H E, Frenner K, Würschum R. *Intermetallics*[J], 1999, 7(3–4): 277
15 Milner D R, Rowe G W. *International Materials Reviews*[J], 1962,7(1): 433
16 Wu X, Shi C, Fang Z *et al. Materials & Design*[J], 2021, 197: 109 279
17 Honarpisheh M, Asemabadi M, Sedighi M. *Materials & Design*[J], 2012, 37(3): 122
18 Miao G. *Transactions of the China Welding Institution*[J], 2020, 41(8): 55
19 Ding J, Cheng Y. *Applied Physics Letters*[J], 2014, 104(5): 611
20 Hla B, Ning L, Tao S *et al. Journal of Materials Research and Technology*[J], 2020, 9(2): 1539
21 Tang Kui, Wang Jinxiang, Fang Yu *et al. Rare Metal Materials and Engineering*[J], 2020, 49(5): 1553
22 Tian X, Wang Z, Teng X *et al. IOP Conference Series Materials Science and Engineering*[J], 2020, 811: 12 013
23 Yw A, Jl B, St B *et al. Journal of Manufacturing Processes*[J], 2018, 36: 417
24 Sherpa B B, Kumar P D, Upadhyay A *et al*. *Propellants, Explosives, Pyrotechnics*[J], 2020, 45(10): 1554
25 Matsuo N, Otuka M, Hamasima H *et al. International Journal of Multiphysics*[J], 2016, 5(2): 131
26 Price M A, Nguyen V T, Hassan O *et al. International Journal for Numerical Methods in Engineering*[J], 2016, 106(11): 904
27 Libersky L D, Petschek A G, Carney T C *et al. Journal of Computational Physics*[J], 1993, 109(1): 67
28 Sparks C, Hinrichsen R, Friedmann D. *46th AIAA/ASME/ASCE/AHS/ASC Structures, Structural Dynamics and Materials*[C]. Texas: AIAA, 2013
29 Zheng Y. *Shanghai Nonferrous Metals*[J], 1991, 12(6): 39
30 Xiao W, Zheng Y Y, Liu H X *et al. Materials & Design*[J], 2012, 35: 210
31 Manikandan P, Hokamoto K, Deribas A A *et al. Materials Transactions*[J], 2006, 47(8): 2049
32 Robinson J L. *Philosophical Magazine*[J], 1975, 31(3): 587
33 Hunt J N. *Philosophical Magazine*[J], 1968, 17(148): 669
34 Cowan G R, Holtzman A H. *Journal of Applied Physics*[J], 1963, 34(4): 928
35 Godunov S K. *Journal of Computational Physics*[J], 1970, 5(3): 517
36 Fu Yanshu, Wang Zhen. *Rare Metal Materials and Engineering*[J], 2018, 47(8): 2458
37 André Koch, Arnold N, Estermann M. *Propellants Explosives Pyrotechnics*[J], 2010, 27(6): 365

基于SPH-FEM算法的爆炸焊接界面参数及波形生长机理研究

吴晓明，史长根，高　立，李文轩，冯　柯
(陆军工程大学，江苏 南京 210007)

摘　要：使用SPH-FEM耦合算法对钛-钢、钢-不锈钢、铜-钢、钛-铝4种常见爆炸复合组合进行了数值模拟，理论分析了材料JC强度方程和SG强度方程的适用应变率范围。探讨了爆炸焊接静态参数基复板厚度和动态参数碰撞速度、动态弯折角对界面温度和压力的影响，借助数值模拟手段研究了界面波形形貌，漩涡和少量飞溅熔化块的生长机理。结果表明，随着复板厚度和碰撞速度的增加，界面温度、压力和波形尺寸明显增加，动态弯折角和基板厚度的改变并不能影响界面温度，界面波形生长遵循着“主逆次顺”运动规律。

关键词：爆炸焊接；界面波形；SPH-FEM；参数研究；强度方程

作者简介：吴晓明，男，1997年生，博士生，陆军工程大学野战工程学院，江苏 南京 210006，E-mail：wuxiaoming@lgdx.mtn